Proceedings of the Institution of Civil Engineers
Geotechnical Engineering 149
July 2001 Issue 3
Pages 167–176

Paper 12394
Received 06/07/2000
Accepted 19/01/2001

Keywords:
codes of practice and standards/ design methods and aids, retaining walls

Robert A. Day
Senior Lecturer, The University of Queensland, Australia

Earth pressure on cantilever walls at design retained heights

R. A. Day

There are many methods for the analysis and design of embedded cantilever retaining walls. They involve various different simplifications of the pressure distribution to allow calculation of the limiting equilibrium retained height and the bending moment when the retained height is less than the limiting equilibrium value, i.e. the serviceability case. Recently, a new method for determining the serviceability earth pressure and bending moment has been proposed. This method makes an assumption defining the point of zero net pressure. This assumption implies that the passive pressure is not fully mobilised immediately below the excavation level. The finite element analyses presented in this paper examine the net pressure distribution on walls in which the retained height is less than the limiting equilibrium value. The study shows that for all practical walls, the earth pressure distributions on the front and back of the wall are at their limit values, K_p and K_a respectively, when the lumped factor of safety F_r is $\leq 2{\cdot}0$. A rectilinear net pressure distribution is proposed that is intuitively logical. It produces good predictions of the complete bending moment diagram for walls in the service configuration and the proposed method gives results that have excellent agreement with centrifuge model tests. The study shows that the method for determining the serviceability bending moment suggested by Padfield and Mair[1] in the CIRIA Report 104 gives excellent predictions of the maximum bending moment in practical cantilever walls. It provides the missing data that have been needed to verify and justify the CIRIA 104 method.

NOTATION

d	length of embedded part of wall or embedment depth
d_o	depth of point O below excavation level
E	Young's modulus of elasticity
F	factor of safety defined by King[2]
F_p	factor of safety on gross passive pressure
F_s	factor of safety on strength
F_r	factor of safety on net available passive resistance
h	height of retaining wall or depth of excavation
I	Cross-section second moment of area
K_a	minimum active horizontal earth pressure coefficient
K_p	maximum passive horizontal earth pressure coefficient
K_0	initial earth pressure coefficient at start of finite element analysis
O	point at which the force R is assumed to act
p_a	horizontal earth pressure at excavation level
p_1	maximum horizontal earth pressure on excavation side of wall
p_2	horizontal earth pressure at bottom of wall
R	net force acting below point O
S	slope of the net pressure distribution below excavation level ($= p_a/x$)
x	depth below excavation level of zero net pressure
y	depth below excavation level of maximum pressure (p_1)
z	depth below original ground surface
ε	depth above bottom of wall of zero net pressure
ε'	$= \varepsilon/d$
γ	bulk unit weight

1. INTRODUCTION

A cantilever sheet pile retaining wall consists of a vertical structural element embedded in the ground below the retained material. The upper part of the wall provides a retaining force due to the wall stiffness and the embedment of the lower part. The embedded cantilever wall obtains its ability to resist the pressure of the retained soil by developing resisting earth pressures on the embedded portion of the wall. Embedded cantilever sheet pile retaining walls are frequently used for temporary and permanent support of excavations up to about 4·5 m high.

The distribution of earth pressure on the embedded part of the wall is dependent on the complex interaction between the wall movement and the ground. Many methods for analysis and design of embedded cantilever walls have been proposed and these have been reviewed by Bica and Clayton.[3] Each method makes various assumptions concerning the distribution of earth pressure on the wall and the deflection or wall movement. Most of the methods are limit equilibrium methods based on classical limiting earth pressure distributions. Model studies on embedded walls have been performed by Rowe,[4] Bransby and Milligan,[5] and Lyndon and Pearson.[6] Bica and Clayton[7] have produced some empirical charts for the design of cantilever walls.

King[3] suggested a semi-analytical limit equilibrium approach for dry cohesionless soil, involving different assumptions from the previous methods. King's method is based on centrifuge test results. Using finite element studies, Day[8] proposed an improvement of King's method for the prediction of the limit equilibrium depth of excavation.

For safety, walls must of course be designed for conditions where the excavation depth is less than the maximum for stability. Fundamentally, the designer needs to assess the earth pressure on the wall and hence the bending moment distribution on the wall at service conditions with the as-built geometry. Current limit equilibrium methods used for calculating the bending moment at service conditions are based on earth pressure distributions assumed to be at their limit values (K_p and K_a) and the use of various factors of safety.

Many authors (e.g. Day,[8] Fourie and Potts[9]) have shown that the earth pressure at the maximum stable height of excavation is closely approximated by a rectilinear pressure distribution. This paper investigates the hypothesis that the earth pressure on cantilever walls in their service condition can also be approximated satisfactorily by a rectilinear pressure distribution, which can be predicted. Thus, the service bending moment distribution is obtainable. It is important to note the subtle difference between this hypothesis and other design methods.[1,10,11] This hypothesis describes the actual earth pressure at service conditions, whereas the design methods do not specifically address the question of the actual earth pressure but give techniques to calculate the design bending moment. A series of finite element analyses of embedded cantilever walls in dry cohesionless soil have been performed to provide data for the study. The recommendations are also compared with the results of a centrifuge model test.

1.1. Design methods

Limit state design philosophy is now commonplace in design codes. The two limit states that are most important for retaining wall design are the ultimate limit state and the serviceability limit state. It is necessary to have accurate analysis tools to enable assessment of these limit states. For structural design of a cantilever retaining wall, the ultimate limit state bending moment is the governing criterion. In some methods, the service bending moment is multiplied by a partial factor or model factor to obtain the ultimate bending moment.[11]

2. ANALYSIS METHODS

The basis of the limit equilibrium methods is the prediction of the maximum height of excavation or the minimum depth of embedment for which static equilibrium is maintained—the limiting equilibrium situation. In this situation, the earth pressure distributions are accurately described by the active and passive limit values (K_a and K_p). This is not the case for the actual design condition. In the design or serviceability situation the distribution of earth pressure on the wall is dependent on the complex interaction between the wall movement and the ground. Also, the earth pressure is such that equilibrium is maintained. Some limit equilibrium methods for determining the design or in-service bending movement are described below.

2.1. Fixed earth method

The earth pressure distribution is simplified as shown in Fig. 1. The lines marked K_a and K_p indicate the active and passive limit earth pressure values. For ease of calculation, the force R, representing the net force acting below the point O, is assumed to act at point O. Moment equilibrium about O yields the value d_o, required for stability. The penetration depth, d, is traditionally taken as $d = 1{\cdot}2d_o$. Finally, a check is made to ensure that

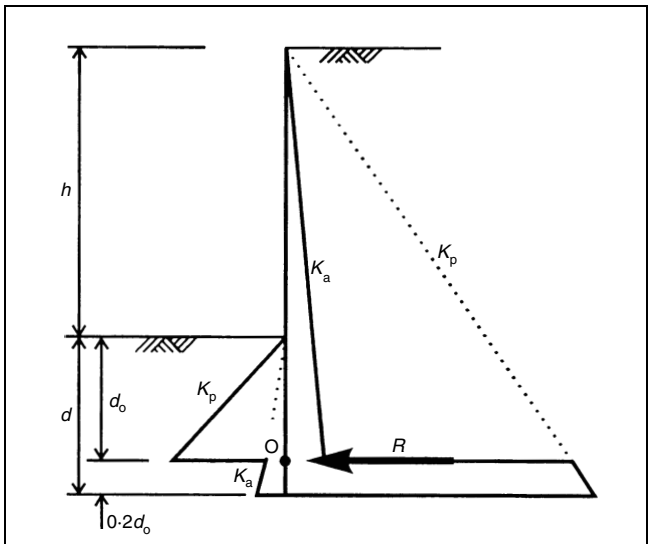

Fig. 1. Simplified pressure distribution

the force R can be mobilised on the wall below point O. Alternately, many software packages do not make these assumptions. The correct location of the force R is used and the extra depth required to develop it is calculated. The bending moment diagram is calculated from the assumed pressure distribution. The following methods have been used to determine the service bending moment.

(*a*) The gross passive pressure is reduced by a factor of safety (F_p) so that with the service geometry and the reduced passive pressure the wall is at a state of limiting equilibrium. The service bending moment distribution is calculated from the resulting factored pressure distribution. This traditional 'working stress' method has now been superseded by the limit state design philosophy.

(*b*) For the given design retained height, the limiting equilibrium depth of embedment is determined using unfactored soil parameters. With this geometry and earth pressure the bending moment distribution is calculated. It is assumed that the maximum bending moment given by this calculation is approximately equal to that actually acting during service in the design configuration. This method is recommended by Padfield & Mair in CIRIA Report 104.[1] It will be referred to in the following discussion as the CIRIA 104 method.

2.2. General rectilinear net pressure method

Day[8] showed that the earth pressure distribution at limiting equilibrium could be approximated by the rectilinear distribution shown in Fig. 2. The rectilinear distribution is characterised by the parameters p_a, p_1, p_2 and y. For a given retained height, h, there are four unknown values (d, p_1, p_2 and y) if the pressure behind the wall at the dredge level, p_a, is assumed to be equal to the active pressure limit. The minimum depth of penetration and the corresponding pressure distribution that just maintains stability (the limiting equilibrium solution) is found from the equations of horizontal and moment equilibrium, and from two assumptions.[8]

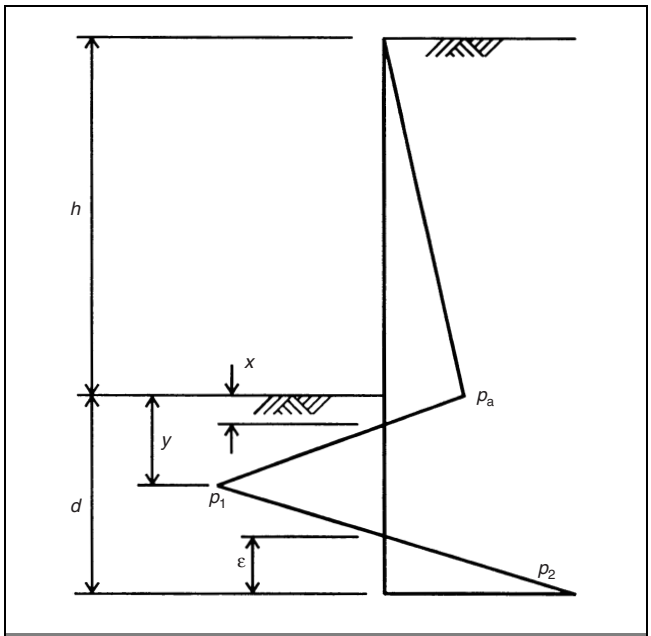

Fig. 2. Rectilinear pressure distribution

(*a*) The limiting passive pressure, K_p, is fully mobilised on the wall immediately below the dredge level. This assumption gives the gradient of the rectilinear pressure distribution between p_a and p_1, which is equal to $\gamma(K_p - K_a)$.
(*b*) Is given by equation (1)

$$\varepsilon' = \frac{\varepsilon}{d} = 0{\cdot}047 \ln\left(\frac{K_p}{K_a}\right) + 0{\cdot}1 \quad (1)$$

For a given wall in the service condition, the embedment depth, d, is known (in the design problem this would have been determined by some other method, such as King's method described above). Thus, only one assumption is needed with the two equations of horizontal and vertical equilibrium in order to obtain the complete pressure distribution (p_1, p_2 and y). King[2] suggested assuming that the value of ε' is constant and equal to 0·35. Other assumptions that could be made include the following.

(*a*) Passive pressure below the excavation level is fully mobilised even when not at the limiting equilibrium geometry.
(*b*) The value of ε' at all stages of excavation is known—but is not necessarily constant.
(*c*) Passive pressure below the excavation level is reduced by a factor, i.e. K_p/F.

3. COMPARISON OF METHODS

3.1. Gross passive pressure method

In the gross passive pressure method, the passive pressure on the wall is reduced by the factor of safety F_p. Hence, the mobilised passive pressure below the excavation level is taken to be K_p/F_p. This is similar to using assumption (*c*) in the rectilinear net pressure method, in which case, the slope of the net pressure distribution between p_a and p_1 is equal to $\gamma(K_p/F_p - K_a)$. For the same value of F, the gross passive pressure and the rectilinear methods (assumption (*c*)) will give the same net pressure and bending moment distribution from the top of the wall to a depth y below excavation level (Fig. 2). Below this point the methods will differ.

3.2. CIRIA 104

The CIRIA 104 method assumes that the maximum bending moment for the design geometry is equal to the maximum bending moment in a wall which has the same retained height but with the limiting equilibrium embedment depth based on unfactored soil parameters. Hence, the maximum service bending moment is independent of the depth of embedment. This implies that in the design geometry, passive pressure is fully mobilised below the excavation level for a depth at least below the point of maximum bending moment. This is similar to using assumption (*a*) in the rectilinear net pressure method. In which case, the slope of the net pressure distribution between p_a and p_1 is equal to $\gamma(K_p - K_a)$. Both the CIRIA 104 and the rectilinear method (assumption (*a*)) will give the same net pressure and bending moment distribution from the top of the wall to a depth y below the excavation level (Fig. 2).

3.3. King's proposal

King[2] suggested for design, a factor of safety, F, defined as

$$F = \frac{x/h}{(x/h)_c} \quad (2)$$

Where c indicates the limiting equilibrium or critical value. At limiting equilibrium when passive pressure is assumed to be mobilised below the excavation level, we can write (Fig. 2)

$$\frac{x}{p_a} = \frac{1}{\gamma(K_p - K_a)} \quad (3)$$

where $p_a = \gamma h K_a$. Hence

$$\left(\frac{x}{h}\right)_c = \frac{K_a}{K_p - K_a} \quad (4)$$

Note that the value of $(x/h)_c$ is dependent on the limiting earth pressures (K_p and K_a) only. It is independent of geometry.

To calculate x/h in the design situation, King suggested using assumption (*b*) and that $\varepsilon' = 0{\cdot}35$. Day[8] showed that a better approximation for ε' at limiting equilibrium is given by equation (1). For the given value of h and the assumed value of ε', the equations of equilibrium can be solved to determine the value of x/h in the design geometry and hence F. From the geometry of the rectilinear pressure distribution, equation (2) and assuming the active pressure is fully mobilised yields

$$\left(\frac{x}{h}\right) = \frac{K_a \gamma}{S} = F\left(\frac{x}{h}\right)_c \quad (5)$$

where $S = (p_a/x)$ is the slope of the line from p_a to p_1. Using equation (4)

$$S = \frac{\gamma(K_p - K_a)}{F} \quad (6)$$

The assumption that ε' is known implies that for retained heights less than the limiting equilibrium height, passive pressure is not fully mobilised immediately below the excavation level.

K_o	1/2				1		2			
Wall stiffness ϕ': degrees	VF*	RF†	RS‡	VS§	RF	RS	VF	RF	RS	VS
20	✓		✓	✓			✓		✓	✓
25			✓							
30			✓							
35	✓	✓	✓	✓	✓	✓	✓	✓	✓	✓
40			✓							
45			✓							
50	✓	✓	✓	✓	✓	✓	✓	✓	✓	✓

*VF = Very flexible
†RF = Reasonably flexible
‡RS = Reasonably stiff
§VS = Very stiff

Table 1. Finite element analyses performed

The slope of the line from p_a to p_1 is given by equation (6), i.e. the net pressure distribution below the excavation level is equal to the limiting net pressure modified by the factor of safety.

4. FINITE ELEMENT ANALYSES

A series of two-dimensional plane strain finite element analyses (Table 1) have been performed to determine the pressure distribution on an embedded cantilever wall when the retained height is less than the limiting equilibrium height. The pressure distributions are compared with the assumed distributions in the limit equilibrium methods described above. In the finite element analyses, the pressure distribution and bending moment were determined by 'excavating' elements from the mesh in front of a 10 m deep wall. Details of the mesh and boundary conditions are shown in Fig. 3. A range of values was assumed for the initial ratio of horizontal to vertical stress in the soil (K_o) before excavation began (Table 1). Analyses by Fourie and Potts[9] and by Day and Potts[12] have shown that the initial value of K_o does not affect the failure height of excavation. This is confirmed by the results of the analyses presented here and by Day.[8] The analyses assume fully drained conditions with pore pressures equal to zero and are therefore applicable to the long-term condition. The Imperial College Finite Element Program was used for the analyses.[13]

An elastic, perfectly plastic cohesionless Mohr Coulomb model was used to describe the soil behaviour. The analyses were performed with various friction angles, ϕ', of the soil ranging from 20° to 50° (Table 1). In each case, the angle of dilation was taken as half the friction angle. The bulk unit weight of the soil, γ, equals 20 kN/m^3. The Young's modulus equals $5000 + 5000z$ kPa, where z is the depth measured from the original ground surface. The Poisson's ratio equals 0·2.

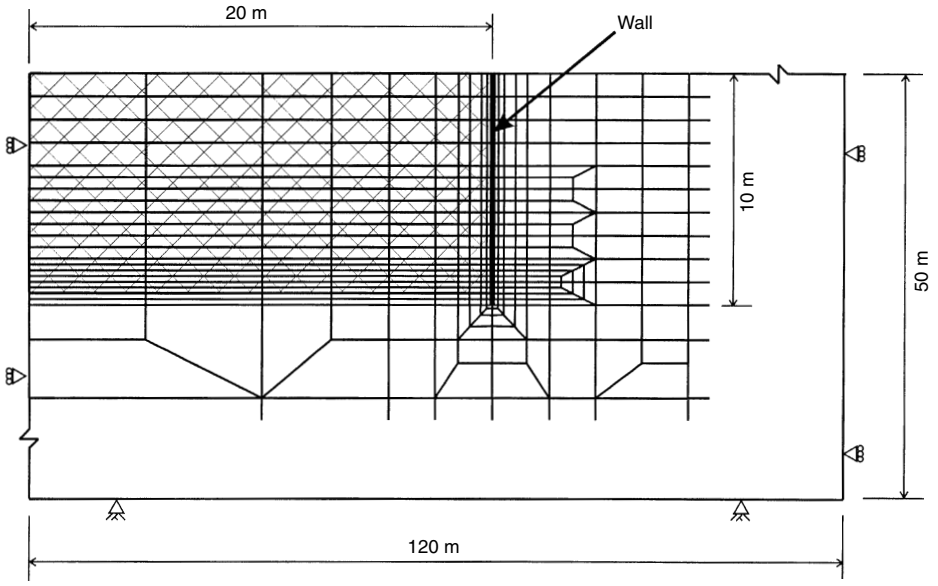

Fig. 3. Finite element mesh (excavated elements hatched)

Designation	Inertia: m^4/m	Area: m^2/m	Stiffness, EI: kNm^2/m
VF	$46{\cdot}8 \times 10^{-6}$	$1{\cdot}13 \times 10^{-2}$	$9{\cdot}8 \times 10^{3}$
RF e.g. 0·3 m minipile @ 0·3 m	$9{\cdot}4 \times 10^{-5}$	$2{\cdot}00 \times 10^{-2}$	$2{\cdot}0 \times 10^{4}$
RS e.g. 1·2 m diaphragm wall	$46{\cdot}8 \times 10^{-4}$	$5{\cdot}26 \times 10^{-2}$	$9{\cdot}8 \times 10^{5}$
VS	$46{\cdot}8 \times 10^{-2}$	$24{\cdot}4 \times 10^{-2}$	$9{\cdot}8 \times 10^{7}$

Table 2. Structural properties of wall

In all analyses, the wall was assumed rough and elastic with Young's modulus = $2{\cdot}1 \times 10^8$ kPa. The analyses covered a range of stiffness values (Table 2). The reasonably flexible and reasonably stiff cases approximately bound the typical range of walls used in practice from lightweight steel sections and mini-pile walls to stiff concrete diaphragm walls. The very stiff and very flexible cases are extreme values.

5. ANALYSIS OF RESULTS

The aim of the finite element analyses was to investigate

whether the rectilinear net pressure distribution is appropriate for the design situation and, if so, could it be defined *a priori*. From the 30 different analyses (Table 1), 96 earth pressure distributions at various stages of excavation have been studied (excluding the limiting equilibrium cases). The rectilinear pressure distribution (Fig. 2) was fitted to the net pressure data points (integration points) obtained from the finite element analyses at each stage of excavation. The rectilinear best fit approximation was found in the following way.

(*a*) The value of p_a was determined using a least squares fit to the bending moment data points above the excavation level. The bending moment was used instead of the stresses because the bending moment is very sensitive to small changes in the pressure.

(*b*) Using this value of p_a, the values of p_1, p_2 and y were determined by a least squares fit of the rectilinear pressure distribution to the finite element net pressure data points over the full wall length. The values of p_1, p_2 and y were additionally constrained so that the net horizontal force and net moment on the wall were zero. The resulting best fit rectilinear net pressure distribution satisfies both moment and force equilibrium. It is a close approximation to the data points obtained from the finite element analyses.

Having determined the best fit rectilinear pressure distribution, the following were determined from the values of p_a, p_1, p_2, y, and the wall geometry, h and d.

(*a*) The mobilised active pressure coefficient, K'_a. In all cases, the mobilised active pressure coefficient K'_a was within a few percent of the theoretical limiting values given by Caquot and Kerisel.[14]

(*b*) The mobilised passive pressure coefficient immediately below the excavation level, K'_p, that is inferred by the rectilinear pressure distribution between p_a and p_1

$$S = \frac{p_a + p_1}{y} = \gamma(K'_p - K'_a) \quad (7)$$

5.1. Earth pressure distribution

Figures 4–7 show the net pressure distribution and corresponding bending moment diagrams for four (of the 96 studied) different cases (Table 3). Also shown on these figures are the pressure and bending moment distributions assumed by King ($\varepsilon' = 0{\cdot}35$), the F_p method and the CIRIA 104 recommendation.

	ϕ': degrees	K_o	Stiffness	h: m	F_r
Fig. 4	35	0·5	VS	5·5	2·73
Fig. 5	50	2·0	VF	7·0	8·84
Fig. 6	50	0·5	VS	8·0	2·45
Fig. 7	50	2·0	VS	7·5	4·94

Table 3. Details of cases shown in Figs 4–7

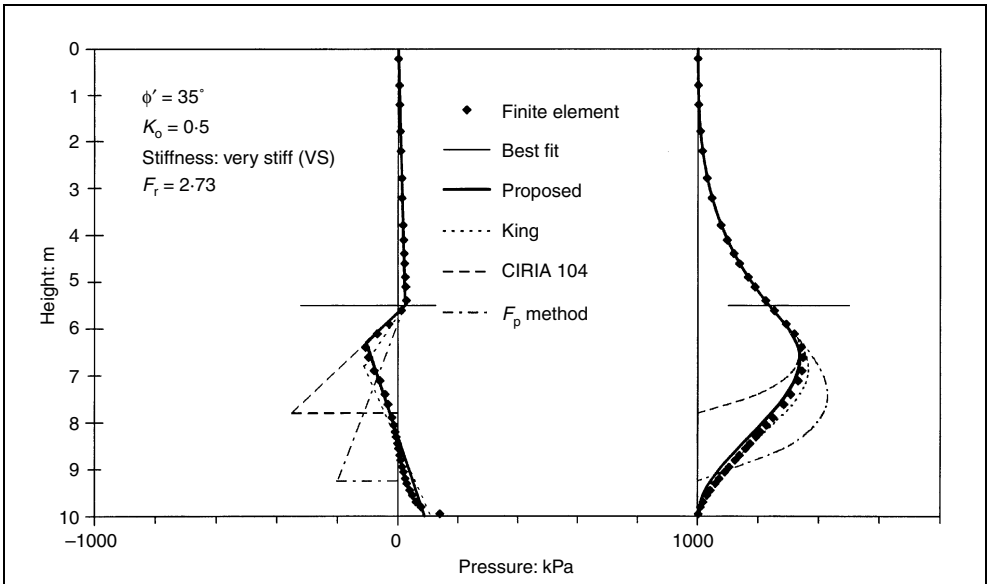

Fig. 4. Net pressure and bending moment distribution—example 1

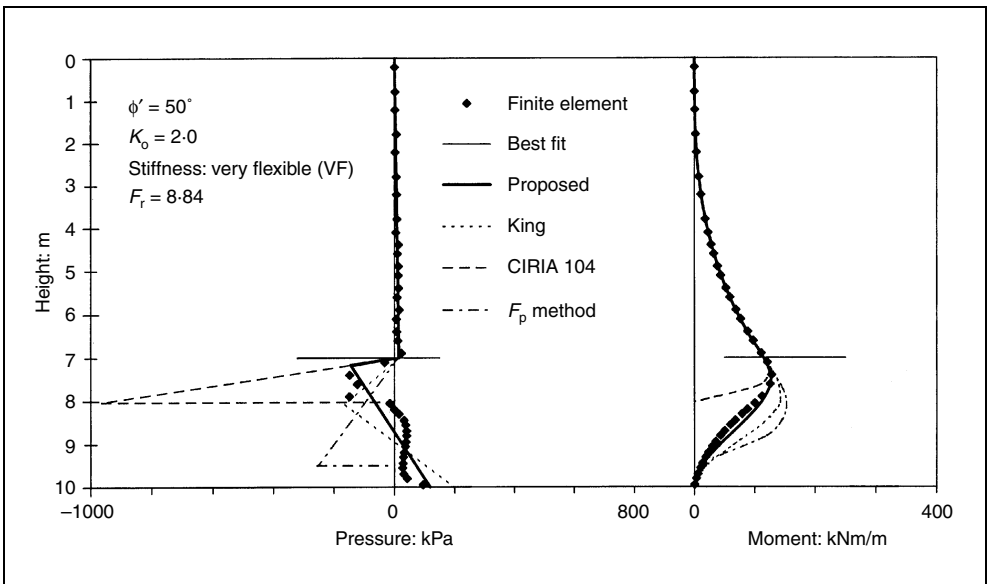

Fig. 5. Net pressure and bending moment distribution—example 2

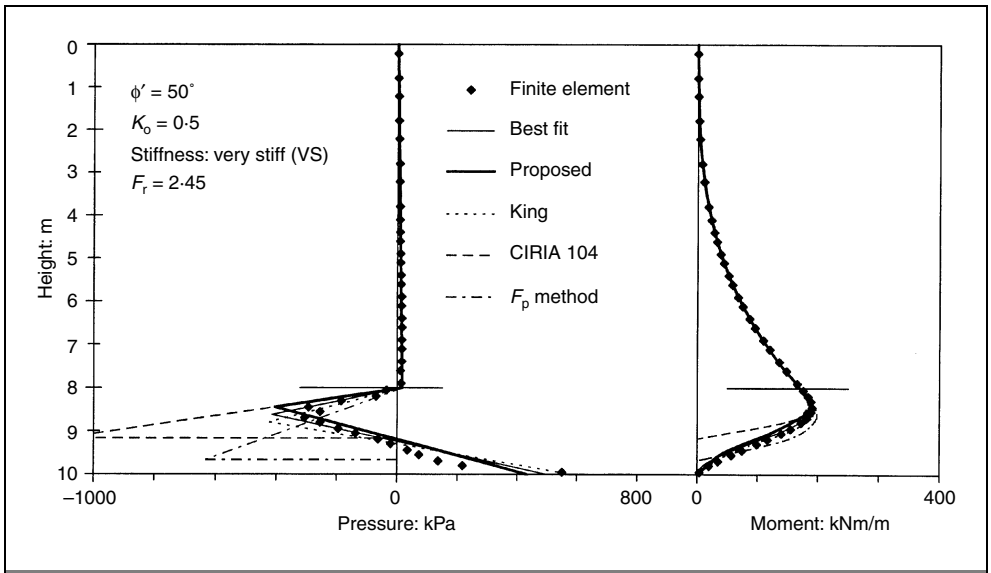

Fig. 6. Net pressure and bending moment distribution—example 3

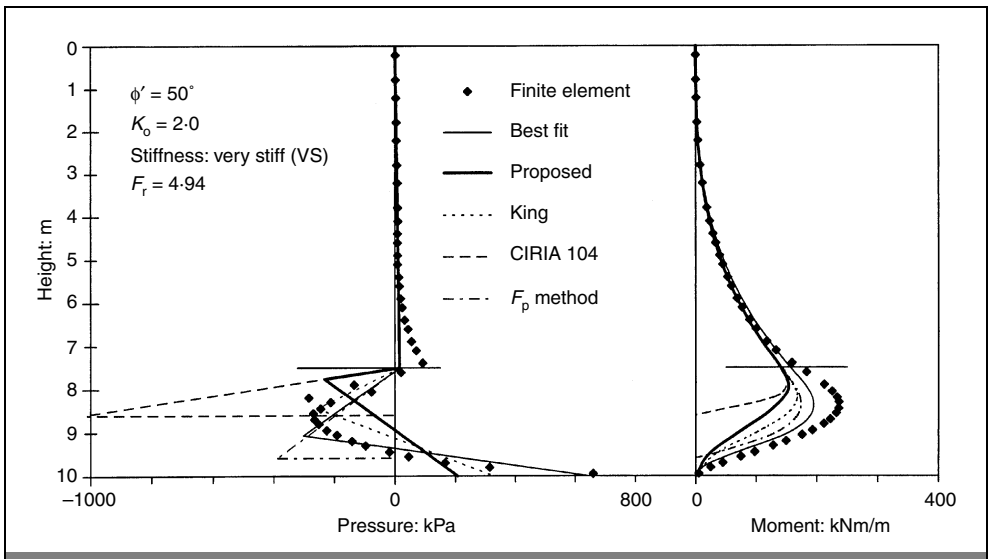

Fig. 7. Net pressure and bending moment distribution—example 4

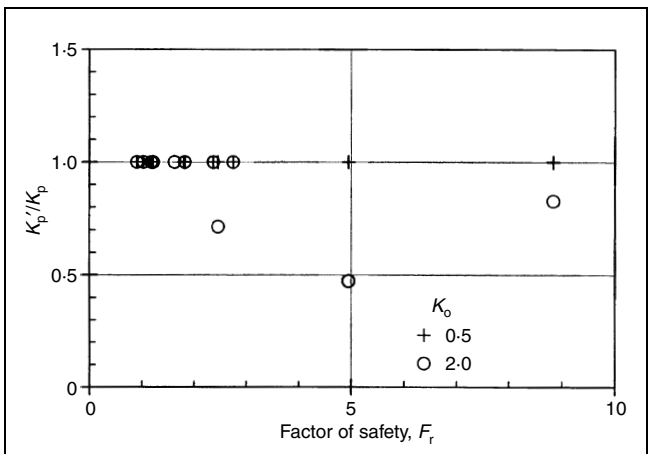

Fig. 8. Mobilised passive pressure—very flexible walls

In the first three cases (Figs 4–6), the best fit rectilinear pressure distribution is a reasonable approximation to the net pressure and gives a very accurate bending moment diagram. In the last case (Fig. 7), the active pressure above the excavation level is non-linear. It increases rapidly a couple of metres above the excavation level. The rectilinear approximation is not appropriate in this case. The deviation of the actual active pressure from the linear assumption results in the maximum bending moment being much greater than that obtained from the rectilinear assumption. The mobilised passive pressure, K_p', obtained from the slope of the line from p_a to p_1, is also not correct. It is underestimated because the calculation is based on the assumption that the pressure on the active side of the wall increases at a rate equal to $\gamma K_a'$. Clearly, this is incorrect. For the case illustrated, the value of K_p' obtained from the rectilinear approximation is 10·3 compared with the value of 26·2 obtained from fitting a straight line to the passive pressure data points. Both values are considerably less than the limiting value of 47·7.[14]

It is useful to examine the results of all of the cases analysed by comparing the mobilised passive pressure K_p' obtained from the best fit rectilinear distribution with the maximum value of K_p given by Caquot and Kerisel.[14] Figs 8–11 show the mobilisation ratio K_p'/K_p plotted against the factor of safety F_r.[15] A mobilisation ratio equal to 1·0 indicates that the theoretical limiting active and passive pressure states are fully mobilised on the wall to some depth below excavation level.

Figure 8 shows the results of all the cases in which the wall is very flexible (VF). Except for three cases with high initial stresses ($K_o = 2{\cdot}0$), it can be seen that the limiting theoretical passive pressure is fully mobilised on the wall ($K_p'/K_p = 1{\cdot}0$) for all excavation levels studied. In the three exceptional cases, the active pressure on the wall was non-linear (e.g. Fig. 7) and thus the value obtained is not appropriate.

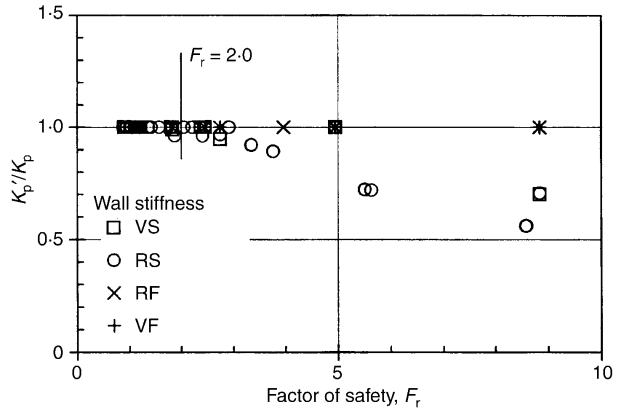

Fig. 9. Mobilised passive pressure—K_o = 0·5

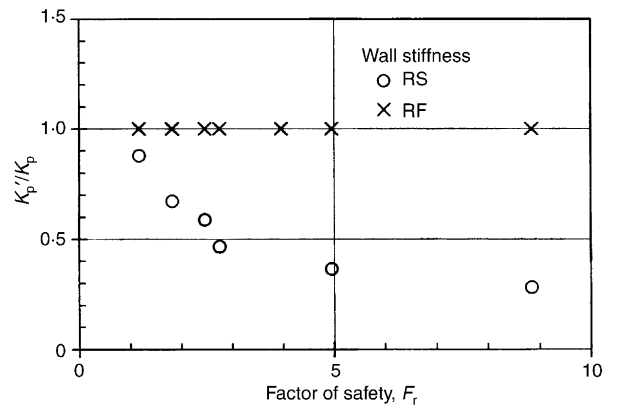

Fig. 10. Mobilised passive pressure—K_o = 1·0

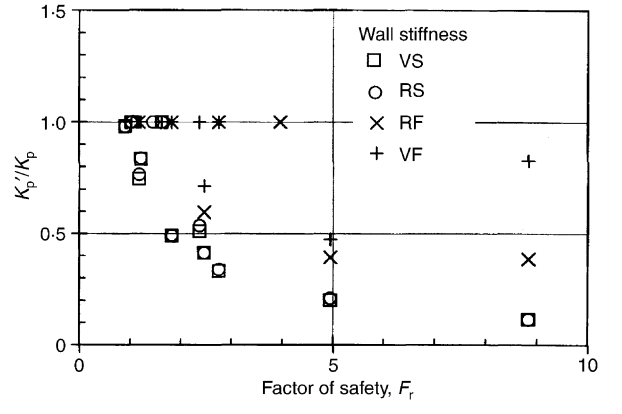

Fig. 11. Mobilised passive pressure—K_o = 2·0

Figure 9 shows the results of all the cases in which the initial stress $K_o = 0{\cdot}5$. In all of these cases, the best fit active pressure was equal to the fully mobilised limiting value given by Caquot and Kerisel.[14] The figure indicates that

- for flexible walls (VF and RF), passive pressure is fully mobilised even at very large factors of safety
- for stiffer walls (RS and VS), as the excavation depth increases towards the limiting equilibrium depth ($F_r = 1$), the mobilisation ratio increases to 1·0.

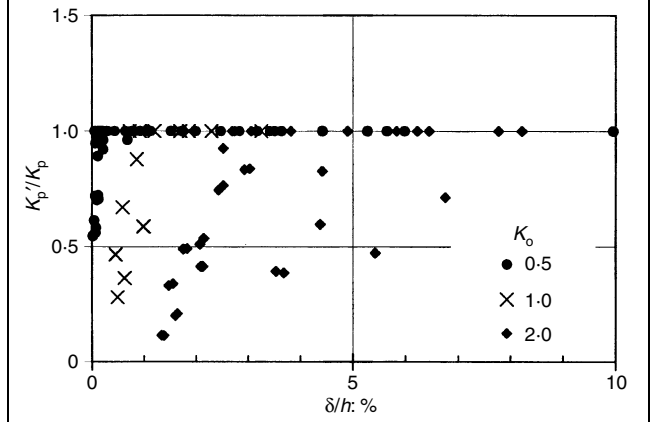

Fig. 12. Displacement of top of wall

For typical design situations, F_r is less than or equal to 2·0, in which case, active and passive pressures are fully mobilised on the wall in the design situation.

Figure 10 shows the results of all the cases in which the initial stress $K_o = 1{\cdot}0$. The figure indicates that for flexible walls (RF) the passive pressure is fully mobilised even at high factors of safety. For stiffer walls (RS), passive pressure is not fully mobilised until excavation is very near to the limiting equilibrium depth.

Figure 11 shows the results of all the cases in which the initial stress $K_o = 2{\cdot}0$. In most of these cases, the active pressure distribution remained non-linear (e.g. Fig. 7) until the factor of safety was less than the typical design values. A linear active pressure distribution did not mobilise until the excavation level was very near the limiting equilibrium depth. However, for some of the very flexible (VF) wall cases the active pressure was full mobilised at high factors of safety (Fig. 5).

5.2. Wall movement

Wall movement is an important consideration for the design of cantilever walls. The movement of the top of the wall, δ, at each excavation level studied is plotted in Fig. 12 against the mobilisation ratio. This figure indicates that, in general, as the movement increases the mobilisation ratio increases. The data points fall into three distinct zones depending on the initial stress. The walls in high K_o soil have large movement ($\delta/h > 1\%$) even when the mobilisation ratio is small. Fig. 12 suggests that a cantilever wall in high K_o soil is unable to control the movement to below acceptable levels. Walls in the low K_o cases are seen to mobilise the full active and passive earth pressures ($K_p'/K_p = 1{\cdot}0$) with acceptable wall movement.

6. DISCUSSION

In typical design situations ($F_r \leq 2$), cantilever walls in low K_o soils will fully mobilise the active pressure distribution on the back of the wall (to a depth below the excavation level) and the full passive pressure distribution on the front of the wall

immediately below the excavation level. The simple rectilinear pressure distribution gives a good approximation to the net pressure and the bending moment. The pressure distribution, and hence bending moment, can be calculated using the two equations of equilibrium and the assumption that passive pressure is fully mobilised below the excavation level.

For cantilever walls constructed in high K_o soils, the active pressure is generally non-linear and the passive pressure is considerably less than the theoretical limiting value (Fig. 7). In these cases, the net pressure and bending moment cannot be determined for the typical design geometry. It is not until very near to failure (Fig. 11) or for extremely flexible walls (Fig. 5) that the rectilinear approximation using assumption (*a*) is suitably accurate. However, in high K_o cases, it is likely that a cantilever wall is unsuitable because the wall movement would be too large.

For all of the very flexible (VF) wall cases (except for three discussed above) the rectilinear approximation assuming full passive pressure below excavation level gives a good estimate of the bending moment distribution in the wall (e.g. Fig. 5). The implication of this is that any ductile wall that is under-designed for a higher bending moment applied to it would yield causing the bending moment to reduce. The assumption of full pressure mobilisation is therefore appropriate in the limit states for strength and stability for all ductile walls.

6.1. Proposed design method

It is proposed that for the design of practical cantilever walls in typical design situations with normal factors of safety (i.e. $F_r \leq 2$), the rectilinear pressure distribution using assumption (*a*) is a good approximation to the net pressure and gives an accurate bending moment diagram. That is

- the active earth pressure is linear with K_a equal to the theoretical value published by Caquot and Kerisel[14]
- the passive earth pressure (K_p) immediately below the excavation level is at the theoretical limiting value given by Caquot and Kerisel.[14]

With these two assumptions and the two equations of equilibrium, the net pressure distribution and the bending moment in the design situation can be determined. The distributions calculated in this way have been plotted in Figs 4–7 for comparison with the finite element data and the other design methods. The proposed method gives excellent predictions.

6.2. Comparison with CIRIA 104

The CIRIA 104 method implies that passive pressure is fully mobilised below excavation depth for an unknown distance. The pressure distributions for the CIRIA 104 method and the proposed methods are the same from the top of the wall to a depth y (Fig. 2) below excavation level. The bending moment at any point in the wall is determined from the forces applied above that point. If the maximum bending moment occurs above the point p_1 (Fig. 2) then the maximum bending moment predicted by the CIRIA 104 method and the proposed method will be equal. If the point of maximum bending moment is below p_1, the CIRIA 104 method and the proposed method will differ. In this case, the CIRIA 104 method gives a value of maximum bending moment that is smaller than the proposed method.

The point of maximum bending moment is typically below the point p_1 at low values of h/d. As h/d increases (F_r reduces), the distance y increases. The maximum bending moment occurs above the point p_1 at higher values of h/d. Fig. 13 shows the ratio of the maximum bending moments calculated from the proposed method (M_p) and the CIRIA 104 (M_{CIRIA}) method. Except for walls with high factor of safety in low strength soils (low K_p/K_a), the two methods differ by only a few per cent. The CIRIA 104 method produces an excellent prediction of the maximum bending moment in typical design situations. A comparison between the proposed and CIRIA methods for a typical case is shown in Fig. 14.

6.3. Comparison with King's method

King proposed that the earth pressure and bending moment at the design geometry could be determined using the rectilinear pressure distribution with the equations of equilibrium and the assumption that $\varepsilon' = 0{\cdot}35$. The equations of equilibrium, assuming various values of ε', give the relationships between x/h and h/d shown in Fig. 15. Also shown in Fig. 15 is the locus of limiting equilibrium points determined from equation (1). It should be noted that at any depth of excavation, the value of

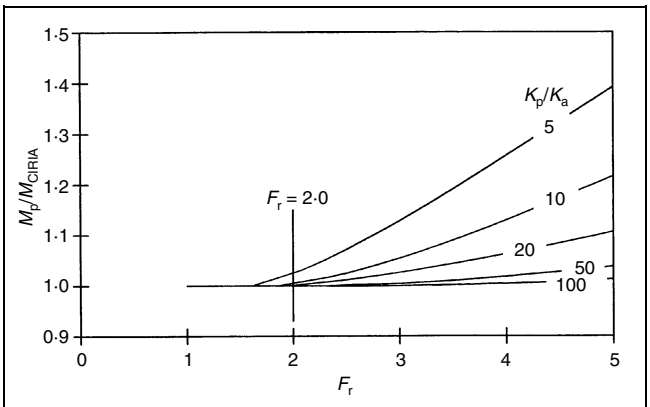

Fig. 13. Comparison of maximum bending moment predictions

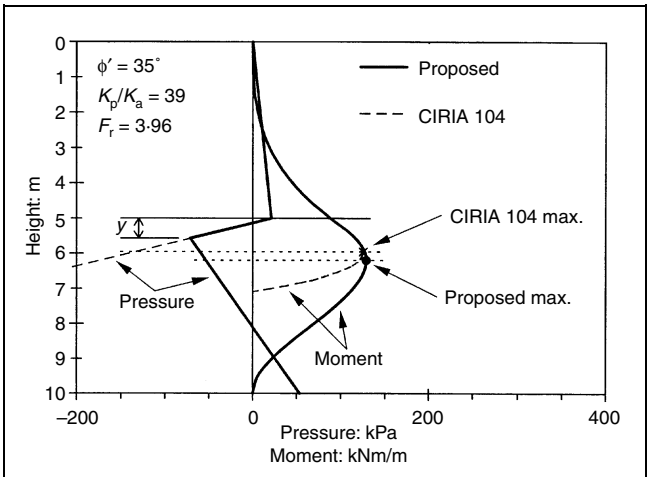

Fig. 14. Comparison of proposed methods and CIRIA 104 method

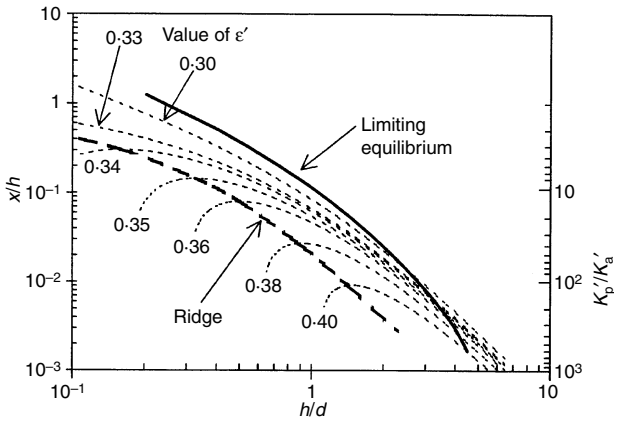

Fig. 15. Equilibrium relationships for the rectilinear net pressure

x/h is dependent only on the ratio of the mobilised pressures K_p'/K_a'. Using equations (3) and (4)

$$\frac{x}{h} = \frac{K_a'}{K_p' - K_a'} \quad (8)$$

The corresponding values of K_p'/K_a' are shown on the right-hand scale of Fig. 15.

King's assumption implies that as h/d increases the stress conditions move along the $\varepsilon' = 0{\cdot}35$ contour to the limiting equilibrium point. Thus, the values of x/h and K_p'/K_a' vary with the excavation depth. However, the results of the finite element analysis indicate that for most practical walls the passive and active pressures are fully mobilised at excavation depths much less than the limiting equilibrium. The value of K_p'/K_a' in the design situation is the same as at the limiting equilibrium. This implies that the value of x/h remains constant as h/d increases. Therefore, the value of ε' will increase and then decrease to the limiting equilibrium point as h/d increases.

6.4. Comparison with King's centrifuge test

Figure 16 shows the bending moment diagram determined by the proposed method compared with centrifuge model test data[2] and the other design methods. The value of F_r for this wall is 3·16. The proposed method matches the experimental data extremely well and is considerably better than the other three methods. For the reasons discussed above, the CIRIA 104 method gives an excellent prediction of the maximum bending moment.

7. CONCLUSION

This study indicates that for practical cantilever walls with typical factors of safety, the active and passive pressure in the design condition can be assumed to be at the theoretical limiting values given by methods such as Caquot and Kerisel.[14]

A rectilinear net pressure distribution comprising three lines provides a good approximation to the actual net pressure distribution and bending moment diagram at excavation depths less than the limiting equilibrium case. This pressure distribution may be calculated using the equations of horizontal and moment equilibrium and the following assumptions

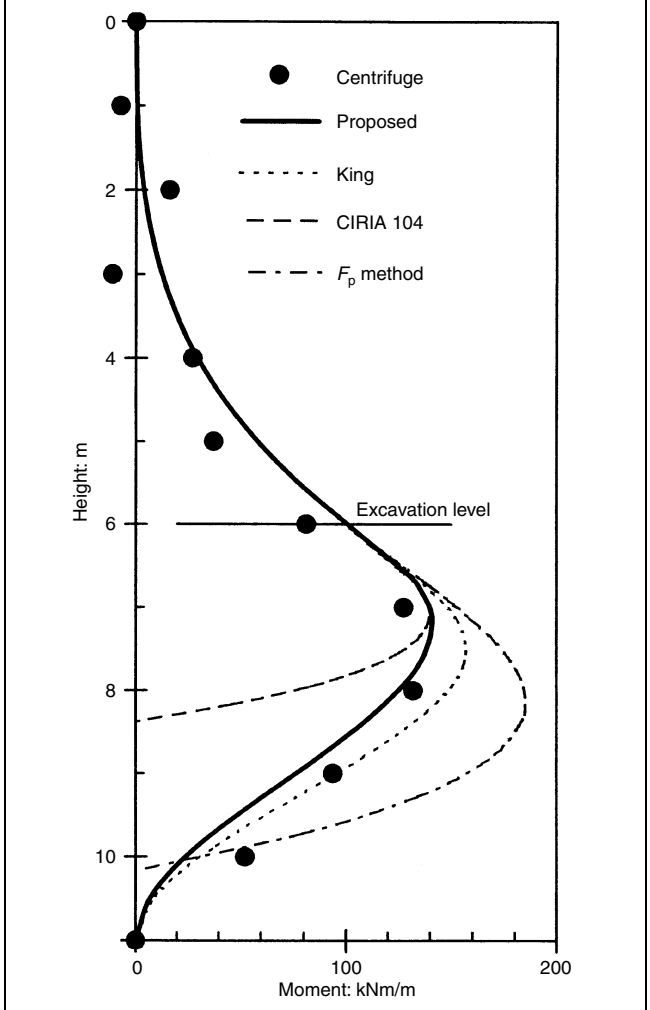

Fig. 16. Comparison with centrifuge model test

- active pressure is fully mobilised above and immediately below the excavation level
- passive pressure is fully mobilised immediately below the excavation level.

The results presented here provide verification and justification of the method proposed by Padfield and Mair in CIRIA Report 104.[1] The CIRIA 104 method gives a very good prediction of the maximum bending moment in the design geometry and the CIRIA prediction is typically in error by less than a few per cent.

The calculation of the maximum bending moment given by the CIRIA 104 method may be simplified. Since the maximum bending moment in a cantilever wall is dependent only on the net pressure above that point, it is not necessary to calculate the limiting equilibrium depth of embedment for the design retained height. The maximum bending moment can be calculated directly using the assumption that the passive pressure is fully mobilised. The maximum bending moment is

$$M_{max} = \frac{1}{6}K_a\gamma(a+h)^3 - \frac{1}{6}K_p\gamma a^3$$

where,

$$a = \frac{h}{\sqrt{K_p/K_a} - 1} \quad (9)$$

REFERENCES

1. Padfield C. J. and Mair R. J. *Design of retaining walls embedded in stiff clays*. Construction Industry Research and Information Association Report 104, 1984, CIRIA, London.
2. King G. J. W. Analysis of cantilever sheet pile walls in cohesionless soil. *Journal of Geotechnical Engineering, ASCE*, 1995, **121**, No. 9, Sept., 629–635.
3. Bica A. V. D. and Clayton C. R. I. Limit equilibrium design methods for free embedded cantilever walls in granular materials. *Proceedings of the Institution of Civil Engineers*, 1989, **86**, Part 1, Oct., 879–989.
4. Rowe P. W. Cantilever sheet piling in cohesionless soil. *Engineering*, 1951, **172**, No. 7, 316–319.
5. Bransby J. E. and Milligan G. W. E. Soil deformations near cantilever retaining walls. *Géotechnique*, 1975, **24**, No. 2, 175–195.
6. Lyndon A. and Pearson R. A. Pressure distribution on a rigid retaining wall in cohesionless material. *Proceedings of International Symposium on Application of Centrifuge Modelling to Geomechanics Design* (ed. W. H. Craig). A. A. Balkema, Rotterdam, pp. 271–280.
7. Bica A. V. D. and Clayton C. R. I. The preliminary design of free embedded cantilever walls in granular soil. In *Retaining Structures* (ed. C. R. I. Clayton), 1993, Thomas Telford, London, pp. 731–740.
8. Day R. A. Net pressure analysis of cantilever sheet pile walls. *Géotechnique*, 1999, **49**, No. 2, 231–245.
9. Fourie A. B. and Potts D. M. Comparison of finite element and limiting equilibrium analyses for an embedded cantilever wall. *Géotechnique*, 1989, **39**, No. 2, 175–188.
10. British Standards Institution. *Code of Practice for earth retaining structures BS 8002:1994*. BSI.
11. *Eurocode 7: Geotechnical design*, ENV 1997-1:1995, CEN, Brussels.
12. Day R. A. and Potts D. M. Modelling sheet pile retaining walls. *Computers and Geotechnics*, 1993, **15**, 125–143.
13. Potts D. M. and Zdravkovic L. *Finite element analysis in geotechnical engineering—theory*, 1999, Thomas Telford, London.
14. Caquot A. and Kerisel J. *Tables for the calculation of passive pressure, active pressure and bearing pressure of foundations*, 1948, Gauthier-Villars, Paris.
15. Burland J. B., Potts D. M. and Walsh N. M. The overall stability of free and propped embedded cantilever retaining walls. *Ground Engineering*, 1981, **14**, No. 5, July, 28–38.

Please email, fax or post your discussion contributions to the secretary: email: kathleen.hollow@ice.org.uk; fax: +44 (0)20 7799 1325; or post to Kathleen Hollow, Journals Department, Institution of Civil Engineers, 1–7 Great George Street, London SW1P 3AA.